

BOUNDARY LAYER DEVELOPMENT ON PAPER DRYING FELTS

S.A. REARDON

Department of Civil & Mechanical Engineering
 University of Tasmania, GPO Box 252C
 Hobart, TAS 7001, AUSTRALIA

ABSTRACT

Boundary layer traverses were performed over a curved hot plate covered by several interchangeable paper drying felts. There was found to be a significant variation in skin friction between the drying felts which are classified in terms of their air permeability and present a fully rough surface to the flow. The results are useful in assessing the aerodynamic behaviour of different felts with regard to their effect on paper sheet instability.

The temperature boundary layer over the smooth curved hot plate was also studied with the aim of defining the heat flux and surface heat transfer coefficient. The latter was found to vary in proportion to the skin friction coefficient.

NOTATION

c_f	skin friction coefficient
c_p	specific heat capacity
k	roughness size
k^+	roughness parameter, ku_s/ν
q_w	heat flux
T	temperature
T_w	wall temperature
T_*	heat transfer temperature
T^+	dimensionless temperature
u	local velocity
u_*	friction velocity
u^+	dimensionless velocity, u/u_*
U_∞	free stream velocity
x	streamwise coordinate
y	coordinate normal to wall
y^+	dimensionless transverse coordinate, yu_s/ν
δ	boundary layer thickness
ρ	density
ν	kinematic viscosity

INTRODUCTION

Paper drying is achieved on a paper machine by passing the sheet over a series of rotating steam heated drying cylinders. During its passage through the dryer section the paper sheet is supported by a number of felt runs. Such felts are typically highly synthetic, monofilament woven fabrics and are categorised in terms of their air permeability.

A study is currently progressing which models the drying rate of paper on an operational paper machine. Relevant to a reliable model is the facility in describing the

effect of the dryer felts on the heat and mass transfers. The degree of air entrained by the moving felt is significant in controlling the transfer parameters and will vary with felt permeability.

The variation in the permeability of drying fabrics through the dryer section run prompts questions concerning their varying aerodynamic behaviour. The amount of air dragged by a fabric whilst travelling through the dryer section at speeds of 15-20 m/s is significant from two points of view. Firstly, the boundary layer profile will influence heat and mass transfer from the paper sheet, through the felt and into the hood air. Secondly, the air layer entrained by the fabric is cyclically pumped into and out of dryer pockets as the fabric negotiates the turning rolls. The air currents generated by this process may cause paper sheet instability. This is undesirable as it may result in paper breaks if the sheet oscillations are significant or encourage sheet wrinkles and folded edges which are forbidden from a quality viewpoint. Figure 1 demonstrates air being entrained by both the dryer fabric and the paper sheet itself.

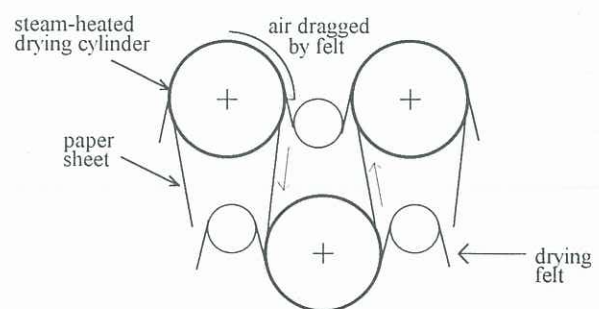


FIGURE 1
 Schematic diagram illustrating air boundary layers generated during the paper drying process.

EXPERIMENTAL SET-UP

An experimental rig comprising a curved hot plate covered by a paper drying felt within a square-sectioned duct, which was previously used for conducting paper drying trials, was modified to allow the boundary layer development across the curved felt section to be investigated. A traversing dial gauge was mounted on rails above the roof of the test duct. A straight-armed hot wire probe and probe support were mounted to the traversing block to allow measurement of both fluid velocity and temperature in the boundary layer

forming over the tensioning fabric. This arrangement is depicted in figure 2.

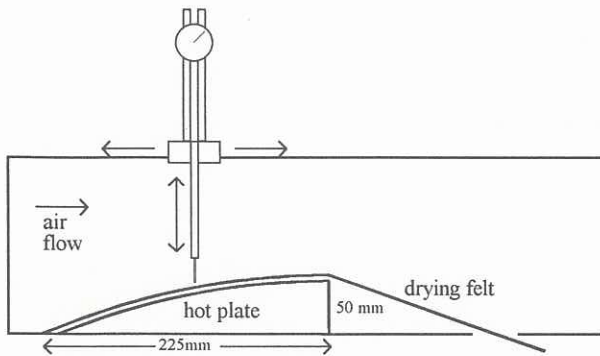


FIGURE 2

Experimental set-up for boundary layer measurements

Velocity boundary layer measurements are made on three different drying felts. Two of these trials made use of actual paper machine drying fabrics with rated permeabilities of 75cfm and 350cfm where cfm is the paper industry ranking in terms of cubic feet per minute of air (at given temperature and pressure) transmitted through the felt under a differential pressure of 1/2" water gauge. The third trial configuration replaces the felt with a number of nylon lines which are tensioned to hold the hot plate in place without disturbing the air flow over the smooth curved surface.

A boundary layer traverse is made at several axial locations along the centreline of the hot plate. Due to the rough nature of the dryer fabric surface it was difficult to physically define a datum for the probe to operate from. The relatively large protrusions of the monofilament polyester weave into the flow demonstrate that the surface datum will necessarily be a somewhat arbitrary definition. This is illustrated by the electron micrograph of figure 3. The zero datum was estimated by extrapolating the linear section of the momentum boundary layer profile to a point where the no-slip condition is satisfied. As velocities as low as $0.1U_\infty$ were able to be measured near the surface the approximation is expected to be satisfactory.

The Mitutoyo dial gauge used for traversing the hot wire probe was calibrated in 0.01mm units and it was possible to take measurements within 0.10mm of the fabric surface. The measured profiles over the dryer fabrics were found to be sufficiently steady to reliably extrapolate the data to the nominal traversing datum. The data obtained from these boundary layer measurements are used to assign skin friction coefficients for the drying fabrics at these locations.

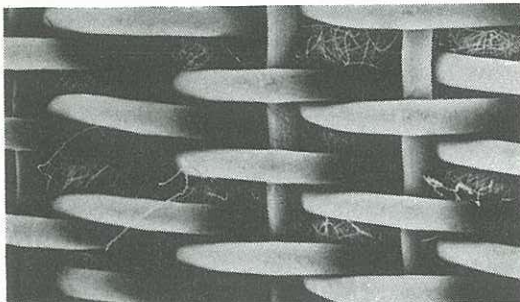


FIGURE 3

Scanning electron micrograph of 75cfm drying felt at a magnification of approximately 10.

The hot wire probe was also utilised to measure the temperature boundary layer above the curved hot plate whilst a thin aluminium backing plate is in contact with it, under tension from a series of nylon lines which acts as a felt substitute. Figure 4 depicts this arrangement which is relevant to the paper drying investigation which prompted this study.

Using the probe as a resistance thermometer enables the temperature layer to be defined. Comparing this profile with other correlations enables the heat flux to be determined. The hot plate temperature is measured with embedded thermocouples and hence the surface heat transfer coefficient can be estimated. This set of data also provides the opportunity to calculate the contact heat transfer coefficient between hot plate and thin backing plate which supports the paper sheet. It is anticipated that the contact heat transfer coefficient should change with felt tension.

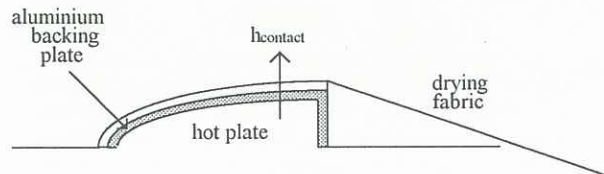


FIGURE 4

Heat transfer between hot plate and a thin aluminium backing plate.

A type 55 P01 constant temperature hot wire probe was used for the boundary layer measurements. It was calibrated over the range 0-20 m/s by a Betz micromanometer which operates with a precision of $\pm 0.1 \text{ mmH}_2\text{O}$. Temperatures were obtained by measuring the probe's resistance at the local conditions and using its temperature coefficient of resistivity to relate this to resistance at standard conditions. For the platinum wire the temperature coefficient of resistivity is $0.0036 / ^\circ\text{C}$.

The average velocity and turbulence intensity through the boundary layer are measured via a channel of the analog-to-digital converter installed in the datalogging computer. Each data point is determined from 10000 samples which are generated from the I/O board at a rate of 600Hz.

RESULTS AND DISCUSSION

As the aim of the study was to differentiate between drying felts on the basis of their aerodynamic behaviour it was considered sufficient to measure velocity profiles and calculate skin friction coefficients at three longitudinal locations along the centreline of the duct. Given that the curved hot plate has an axial span of 225mm, the measurement sites were selected as 5mm, 115mm and 225mm relative to the leading edge. Results were obtained at a Reynolds number of 2.5×10^5 .

Velocity Profile

Figures 5a, 6a and 7a show the wall law relationship of $u^+ \sim y^+$ for each of the three axial positions whilst figures 5b, 6b and 7b demonstrate the normalised axial RMS velocity profile for the various surfaces.

Baskaran et al (1987) demonstrated the growth of an independent internal boundary layer over a curved hill. The internal layer was found to form as a result of the sharp change in surface curvature at the leading edge of the rise and was seen to control the skin friction distribution.

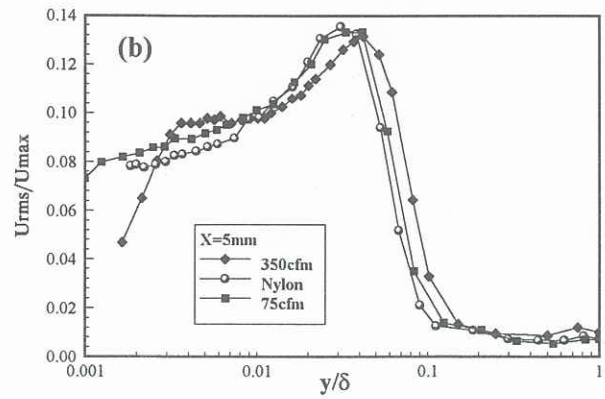
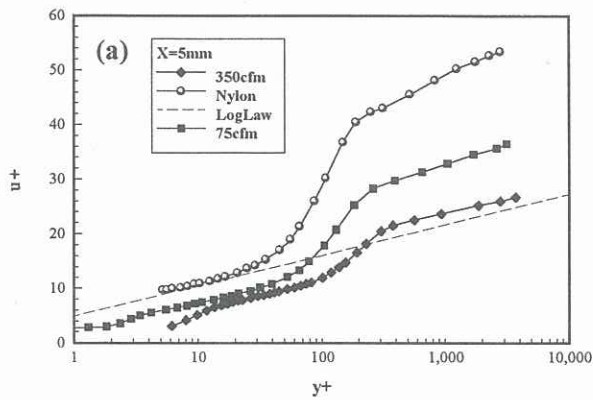


FIGURE 5

Velocity profiles for the three felt arrangements at axial position $x=5\text{mm}$: (a) wall law plot, (b) turbulence intensity

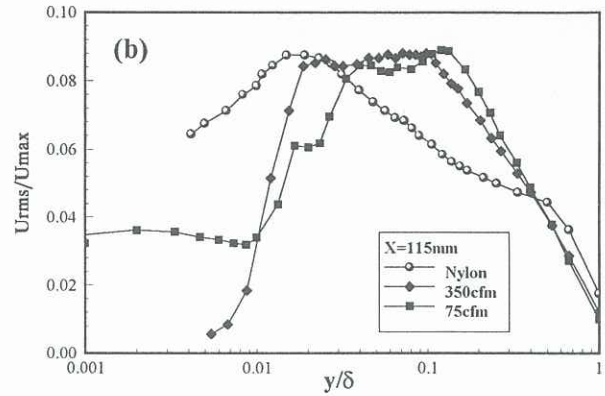
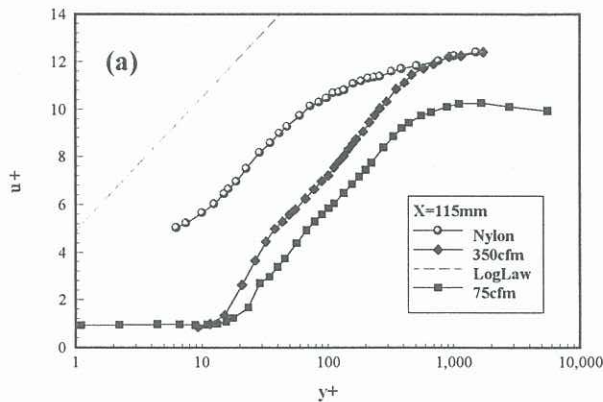


FIGURE 6

Velocity profiles for the three felt arrangements at axial position $x=115\text{mm}$: (a) wall law plot, (b) turbulence intensity

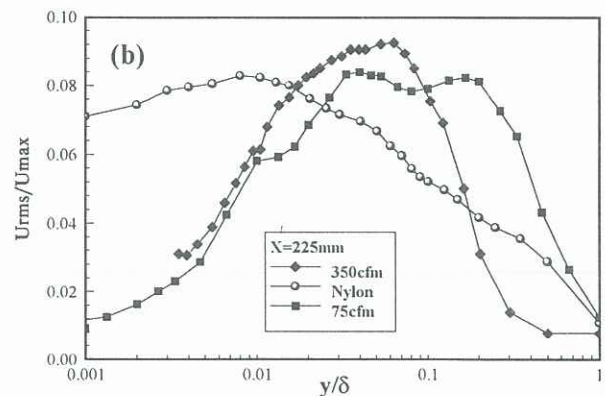
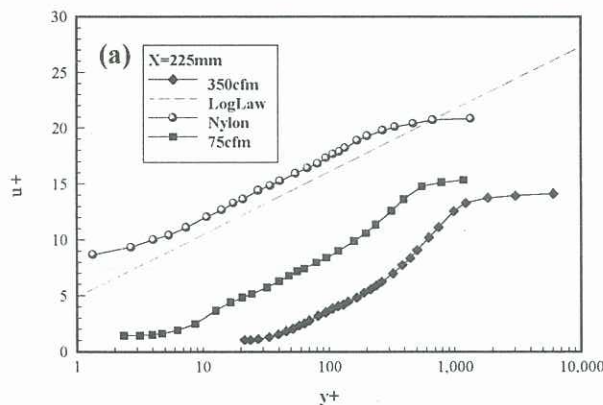


FIGURE 7

Velocity profiles for the three felt arrangements at axial position $x=225\text{mm}$: (a) wall law plot, (b) turbulence intensity

The wall law plot for the roughened felt surface showed a dual slope characteristic after an initial low turbulence parabolic region. The internal layer lies in the range $50 < y^+ < 300$ where the du^+/dy^+ value is independent of surface roughness. By using Clauser's (1956) data for the inner region of the boundary layer with an additive term for surface roughness the law of the wall becomes,

$$u^+ = 5.6 \log(y^+) + 4.9 + 5.6 \log(k^+) + C, \quad (1)$$

where C is a constant and k^+ is the roughness parameter.

The velocity profiles are plotted using an appropriate value of C in the y^+ and u^+ calculations. C is selected so that

the experimental results exhibit the Clauser slope in the internal wall-dominated layer. The resultant skin friction coefficients are listed in Table I.

The axial variation of skin friction coefficient is consistent with the findings of Baskaran et al where C_f is a minimum near the leading edge of the curved hill and increases sharply to a peak at a position $1/3$ the distance along the hill profile before decreasing slowly as the axial position nears the crest.

The variation in C_f between the 75cfm felt, the 350cfm felt and the aluminium plate surface is similar at each axial location and this trend indicates that the more permeable

TABLE I
Skin friction coefficients (Cr) and offset (Δ) for various drying felt and axial location combinations

Axial location x (mm)	No felt		75 cfm		350 cfm	
	Cr	Δ	Cr	Δ	Cr	Δ
5	0.0007	0.6	0.0015	-7.5	0.0028	-4.7
115	0.0130	-5.0	0.0190	-10.3	0.0360	-12.1
225	0.0046	1.4	0.0085	-3.1	0.0100	-12.4

350cfm felt induces more drag than does the 75cfm felt. This result is not obvious from an inspection of the two materials but in hindsight can be attributed to the weave pattern. The 350cfm felt is more porous and the surface comprises a number of relatively isolated roughness elements as opposed to the denser 75cfm felt which presents a more uniform surface.

The turbulence intensity measurements are useful in indicating the proximity of the probe to the rough ill-defined felt surface. Whilst a formal laminar sublayer is not identifiable due to the excessive roughness ($k^+ \approx 60$ for 350cfm felt at $x=225\text{mm}$) the RMS velocity must tend towards zero at the wall. The variation of U_{rms}/U_∞ for small values of y/δ assists in defining zero surface datum for the two rough felts studied. It should be noted that no laminar sublayer was observable in flow over the smooth aluminium hot plate surface which maintained significant turbulence to within approximately $20\mu\text{m}$ of the wall for each trial.

Temperature Profile

Just as Clauser's data were used to determine the skin friction coefficient by equating gradients in the inner region so can Kader's (1981) correlation for the temperature law of the wall assist with defining the heat flux through the surface. This will then form the basis for calculating the desired heat transfer coefficients.

Defining a heat transfer temperature, T_* , of,

$$T_* = \frac{q_w}{\rho c_p u_*} \quad (2)$$

which is analogous to the friction velocity u_* , the dimensionless temperature T^+ becomes,

$$T^+ = \frac{T_w - T}{T_*} \quad (3)$$

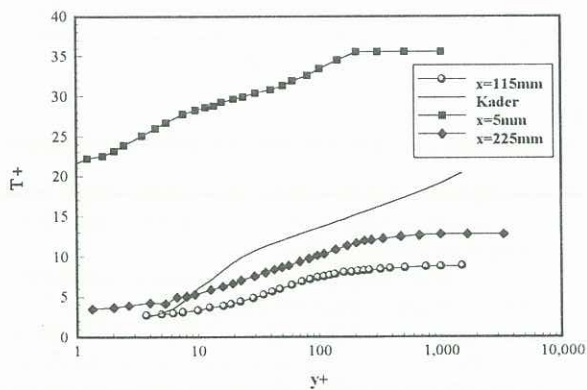


FIGURE 8
Temperature boundary layer profile at three axial locations for the curved hill with no drying felt. Comparison is made with Kader's flat plate correlation.

For air with a Prandtl number of 0.7 over the temperature range studied, the logarithmic region may then be expressed by,

$$T^+ = 4.88 \log(y^+) + 3.73. \quad (4)$$

The temperature profiles for each of the three axial locations are illustrated in figure 8. The associated heat flux, q_w , for each case is quoted in Table II. These data were determined by manipulating the T_* value for each trial to match the gradient of Kader's correlation in the internal wall dominated region. The surface heat transfer coefficient is subsequently derived.

Von Karman's (1939) approximation for turbulent flow over a flat plate showed the surface heat transfer coefficient to be directly proportional to the skin friction coefficient. This trend is evident from comparison of Tables I and II for each of the three felt arrangements.

TABLE II
Heat flux and heat transfer coefficients along the centreline of the hot plate surface.

Location x(mm)	5	115	225
q_w (W/m ²)	1110	16610	8900
($T_w - T_{now}$) (°C)	55	67	95
$h_{surface}$ (W/m ² °C)	20	248	94

The heat flux data presented in Table II also bears application in determining the contact heat transfer coefficient between the hot plate and the thin aluminium backing plate which is an important parameter in controlling the paper drying trials which are proceeding in parallel with this study.

ACKNOWLEDGEMENTS

This work is supported by Australian Newsprint Mills Limited, Boyer, Tasmania.

REFERENCES

BASKARAN, V., SMITS, A.J. and JOUBERT, P.N. (1987), A turbulent flow over a curved hill. Part 1. Growth of an internal boundary layer, *J. Fluid Mech.*, **182**, 47-83.
 CLAUSER, F.H. (1956), *Advances in applied mechanics - Vol. IV*, Academic Press, New York.
 KADER, B.A. (1981), Temperature and concentration profiles in fully turbulent boundary layers, *Int. J. Heat Mass Transfer*, **24**, 1541-1544.
 SCHETZ, J.A. (1984), *Foundations of boundary layer theory for momentum, heat and mass transfer*, Prentice-Hall, Englewood Cliffs, N.J.